HOT SPOTS IN CYGNUS A AT 89 GHz

MELVYN WRIGHT
Radio Astronomy Laboratory, University of California, Berkeley

AND

MARK BIRKINSHAW
Cavendish Laboratory, University of Cambridge
Received 1983 October 17; accepted 1983 December 8

ABSTRACT

The Hat Creek interferometer was used at 89 GHz to map the radio source Cygnus A (3C 405) to a resolution $1''5 \times 2''8$. The hot spots in the radio lobes have straight spectra with spectral indices 0.98 ± 0.02, significantly flatter than the lobe emission of 1.34 ± 0.05. No features corresponding to electron aging have been found in the hot spots. The central component has a flux density of 0.7 ± 0.07 Jy. There is no evidence for 89 GHz variability of the central component over the 10 month interval of this synthesis. The spectrum of the central component is well fitted by a simple model based on the VLBI structure, with core and jet magnetic fields less than about 1 mT.

Subject headings: galaxies: jets — galaxies: structure — radio sources: galaxies

I. INTRODUCTION

The structure of Cygnus A (3C 405) at centimeter wavelengths is well known (e.g., Hargrave and Ryle 1974, 1976; Dreher 1979, 1981) to consist of a central, flat-spectrum component associated with a 15 mag cD galaxy at redshift 0.0567 (Spinrad and Stauffer 1983) with bright, extended radio lobes containing embedded, high-brightness, arcsec-scale hot spots to either side. High dynamic range maps made recently with the VLA (Perley 1983) have shown that a large-scale, thin "jet" lies between the radio nucleus and the Np lobe. VLBI data also demonstrate an extension in this direction (Kellermann *et al.* 1981; Linfield 1982). This observational picture is usually interpreted in the context of the beam model of radio sources (reviewed in Blanford and Rees 1978), where the VLBI and large-scale jets trace the passage of a flow of material from the nucleus to the lobes, and the hot spots are interpreted as regions where this beam meets a dense extragalactic medium in a strong shock.

Further information on the applicability of this model can be obtained by a spatially resolved study of the spectrum of the source. It might be expected that one hot spot in each lobe, where particle acceleration is currently active, should show a flatter spectrum than the remainder of the lobe. High-resolution studies of the source over a wide range of frequencies should therefore provide information on the sites of electron acceleration, and the rapidity of electron aging in any flow away from the hot spots (e.g., Winter *et al.* 1980), and may hope to locate breaks in the emission spectra corresponding to the duration of acceleration in hot spots. Furthermore, the spectrum of the central component should show features associated with the opacity of the synchrotron-emitting material, and possibly also features due to the energy limits in the electron spectrum (Kafatos 1978).

High-frequency single-dish observations of Cygnus A have suggested that the central component has a significantly inverted and complicated spectrum (e.g., Kafatos *et al.* 1980). The low 86 GHz flux density for the central source found by Birkinshaw and Wright (1982) is inconsistent with this view. The central source might be time variable but it is likely that the single dish data have insufficient angular resolution to allow an unambiguous separation of the flux densities of the different components of Cygnus A. Reliable high-frequency spectra for the central component and hot spots of Cygnus A therefore require high-resolution observations, and hence we have made radio synthesis observations of the source at 89 GHz ($\lambda = 3.3$ mm) using the Hat Creek interferometer (Welch *et al.* 1977).

II. OBSERVATIONS

Observations of Cygnus A were made during the period 1982 July to 1983 May using the millimeter interferometer at the Hat Creek Observatory (Welch *et al.* 1977). Observations centered on the position of the nuclear radio source (as given by Hargrave and Ryle 1974) were made at 10 east-west interferometer spacings at equal intervals of 30.5 m from 30.5 to 305 m. At each spacing the interferometer baseline was determined to an accuracy ~ 0.1 wavelength by observing about 20 unresolved sources with well-determined positions over a wide range of hour angles and declinations. Cygnus A was observed for two 12-hour periods at each spacing, with instrumental phase calibrations against the unresolved source 2005+403 (assumed position 1950.0 R.A. = $20^h05^m59^s560$, decl. $40°21'01''80$) at intervals of ~ 30 min.

The instrumental gain and atmospheric extinction were calibrated by a sky-ambient chopper every 10 min, and the flux density scale was determined from observations of Venus using the brightness temperatures given by Ulich (1981). Gain variations in one of the antennas limit the accuracy of the flux density scale to around 10%, of the same order as the likely flux density scale error between the mm-wavelength (Ulich 1981) and cm-wavelength (Baars *et al.* 1977) flux density scales.

Since the radio lobes extend over 2', particular care was taken with the pointing of the 6 m antennas (FWHM = $2'2$). This was done by separately checking the pointing on each antenna while observing 3C 345 (1641+399) with the interferometer. Data with pointing errors exceeding 30" were rejected. The residual pointing errors on a number of sources including

3C 345 were 12″–15″ rms. The effect of random pointing errors in each antenna is to decrease the forward gain and increase the effective size of the polar diagram, and this effect was included in the primary beam correction.

These observations were made with a wide-band (400 MHz) receiver which has a noise temperature at 89 GHz of 120 K. In order to map the whole field without bandwidth decorrelation (e.g., Fomalont and Wright 1974), the observations of Cygnus A were made in a single-sideband mode by offsetting the frequencies of the first and second local oscillators. The rejection of the unwanted sideband is better than 99%. The phase calibrator, 2005 + 403, was observed in the normal double-sideband mode to obtain the best signal-to-noise ratio. The relative phases of the two sidebands were measured and aligned at intervals of approximately 2 hours. Residual errors in the calibration may produce systematic amplitude errors of 10% and phase errors of 10 degrees in the visibility data.

These observations were made with linearly polarized feeds which did not track the parallactic angle, since the antennas of the Hat Creek interferometer are altazimuthally mounted and the feeds cannot be rotated during 89 GHz operation. The rotating linearly polarized flux from the radio lobes might be expected to degrade the synthesis maps of the source, and to lead to a systematic error in the flux density scale. In order to determine the importance of this effect, additional observations with circularly polarized feeds were made in 1983 June at a 30.5 m EW spacing to measure the polarization of the radio lobes of Cygnus A. The instrumental polarization of the crossed circular feeds was measured on Venus.

III. RESULTS

After correction for an instrumental polarization of 4% of the total intensity, the polarization observations were Fourier transformed and combined into maps of the four Stokes parameters. A single spacing of the interferometer suffices to separate the radio components and indicates linear polarizations ≤10% in each of the radio lobes. The position angles are consistent with those measured at 23 GHz (Dreher 1979).

Visibility data for the 10-spacing observations with linearly polarized feeds were convolved onto a 256 × 256 array and Fourier transformed. The FWHM size of the synthesized beam was 1.″5 in R.A. by 2.″8 in decl., with a peak sidelobe level of 6%. The synthesized map was CLEANed (Hogböm 1974) by iteratively subtracting the corresponding synthesized beam response from three boxes containing the outer lobes and the central radio source. For comparison, a maximum
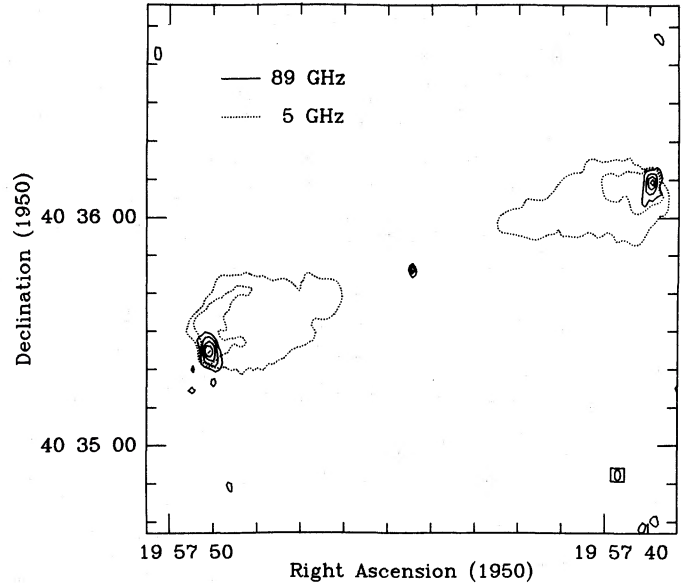
FIG. 1.—The CLEANed map of Cygnus A at 89 GHz, corrected for primary beam. Contours are drawn at equal intervals of 0.2 Jy per synthesized beamwidth, and the half-power beamwidth is shown in the enclosed box. Dotted lines trace the contours of the emission at 5 GHz (from Hargrave and Ryle 1974).

entropy map made using the algorithm of Gull and Daniell (1979) was also computed.

The CLEANed map of the whole field of view of the antenna is shown in Figure 1. The rms noise level on this map is 40 mJy close to the map center, rising to 80 mJy near the radio lobes where the primary beam correction is a factor 2. The dynamic range on the map is determined by residual amplitude and phase calibration errors in the data rather than by receiver noise, and only features on the map brighter than about 10% of the brightest component before the primary beam correction are believable. In order to study the effect of the nonrotating linearly polarized feeds, visibilities were computed for a model source with 10% linearly polarized components, Fourier transformed, and CLEANed in the usual way. Three percent flux-density errors occurred in the resulting maps. Since this error is of the same order as the dynamic range in the 89 GHz map, we will ignore the effect of polarization in the following discussion.

Sizes and flux densities were determined by fitting Gaussian components to the CLEAN map and are summarized in Table 1. The errors in the flux densities include a contribution

TABLE 1

OBSERVED PROPERTIES OF THE RADIO COMPONENTS OF CYGNUS A

Component	R.A. (1950.0)	Decl. (1950.0)	Flux density (Jy)	Angular Size (arcsec)
A	$19^h57^m38^s.965 \pm 0^s.010$	$40°36'09.''3 \pm 0.''3$	1.9 ± 0.2	2.6×4.6
B	19 57 39.12 ± 0.05	40 36 06.1 ± 0.5	0.4 ± 0.1	>4.0
Central	19 57 44.425 ± 0.010	40 35 46.15 ± 0.2	0.70 ± 0.07	<2.0
D	19 57 49.07 ± 0.010	40 35 24.8 ± 0.3	4.2 ± 0.43	3.0×5.3
Np lobe	...	...	4.3 ± 0.6	5.5×3.0
Sf lobe	...	...	7.8 ± 0.8	6.0×3.5
Total	...	...	12.8 ± 1.3	126×6
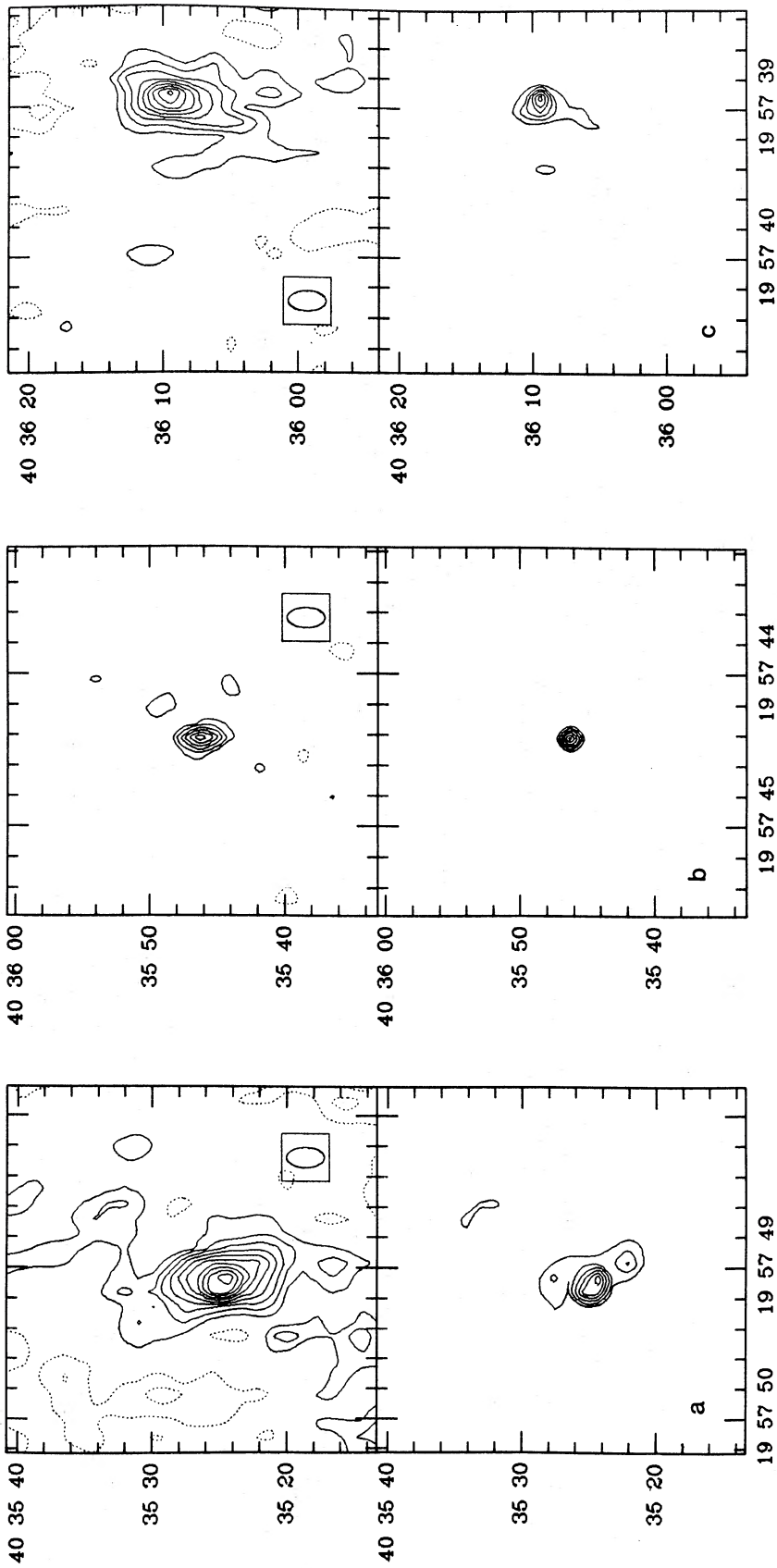
Right Ascension (1950)

FIG. 2.—CLEANed and maximum entropy images of the radio components of Cygnus A. The CLEANed maps (*upper panel*) are contoured at intervals of 0.1 Jy per beamwidth, and the maximum entropy maps (*lower panel*) are contoured at intervals of 15% of the peak brightness in the corresponding component. (*a*) The SF lobe. (*b*) The central component. (*c*) The Np lobe.

from the uncertainty in the absolute flux density scale. Consistent values for the flux densities of all the components were obtained from maps made with partial data sets throughout the 10 month observing period. The central radio source is unresolved with a flux density 0.70 ± 0.07 Jy. The Sf hot spot (Fig. 2) shows a resolved ridge along position angle 16°, with a small remnant of the more extended structure seen at 5 GHz (Hargrave and Ryle 1974) to the NW. The total flux of this component is 7.8 Jy, with 4.2 Jy coming from the inner resolved ridge whose deconvolved size is $3\rlap{.}''0 \times 5\rlap{.}''3$. The Np radio lobe is composed of two hot spots designated A and B by Hargrave and Ryle (1974). Component A is resolved with an integrated flux of 1.9 Jy and a deconvolved size $2\rlap{.}''6 \times 4\rlap{.}''6$. Component B is not well resolved on our map, but appears as a 5% peak at the end of the ridge extending to the SE from component A. Including the extended emission to the east, the total flux from component B is 1.3 Jy. The integrated flux of the NW lobe is 4.3 Jy. The flux densities and angular sizes of these structures are collected in Table 1.

Following Gull and Daniell (1979), the maximum entropy map represents the smoothest distribution of radio flux density consistent with the data. Since the structure of Cygnus A is known *a priori* to be that of a central component with outer radio lobes, our maximum entropy images (Fig. 2) were deduced from a prior distribution consisting of three 30″ half-power full-width Gaussian sources centered on these components superposed on the usual uniform map. The resulting images may be interpreted strictly as the flux-density normalized probability distributions of emission from these regions: thus the central source appears as a circularly symmetric structure (Fig. 2b) with 99% of the flux density within a circle of 1″ diameter, and hence we may deduce with 99% certainty that this component is smaller than 1″. Similarly, components A and D are inconsistent at the 99% level with the hypothesis that they are point sources.

IV. DISCUSSION

Our synthesis maps (Figs. 1 and 2) refer to regions of higher magnetic fields, or of more energetic electrons, than those sampled in earlier maps, made at lower frequency. A comparison of the morphologies of the hot spots at 89 GHz (Fig. 2) and 15 or 23 GHz (Hargrave and Ryle 1976; Dreher 1979), however, shows that little change in morphology occurs over the range 15–89 GHz. Thus it appears that electrons with energies a factor ∼3 higher than those sampled in lower-frequency maps are colocated and coeval.

The total flux density in our map, 12.8 ± 1.3 Jy, is consistent with the peak visibilities seen on our shortest interferometer baseline, and agrees with the flux density 11.6 ± 0.3 Jy predicted from an extrapolation of the spectrum of Cygnus A given by Janssen, Golden, and Welch (1974). Spectra for the principal components of Cygnus A at frequencies above 1 GHz are collected in Figure 3, reduced to the flux density scales of Baars *et al.* (1977) and Ulich (1981) at frequencies below and above 35 GHz, respectively. In the case of component B, the spectrum contains the flux density of the "tail" component apparent on the map of Dreher (1981), since our map has insufficient resolution to distinguish it from the head.

The spectra of hot spots A, B, and D (Fig. 3), are straight in the range 2.7–89 GHz to within the errors, with spectral indices of 1.03 ± 0.05, 1.20 ± 0.07, and 0.93 ± 0.04, respect-

ively. The equipartition magnetic fields in the hot spots are ∼30 nT, so that the synchrotron lifetime for electrons radiating at 89 GHz is only $\sim 3 \times 10^4$ yr. Since the hot spots show no high-frequency spectral curvature, the electrons which radiate at 89 GHz must be able to diffuse across the hot spots (of size ∼3 kpc) in this 3×10^4 yr, corresponding to a diffusion speed of about $0.3c$.

The diffuse emission in the lobes has a steeper spectrum than that of the hot spots. Little of the flux density of Cygnus A can be lost on our map, since structure on scales less than 10″ is well sampled, and so we may estimate accurately the flux densities of the diffuse lobe emission at 89 GHz from our data. In order to improve the signal-to-noise ratio, the flux densities from the two lobes were added, and the overall spectrum of the diffuse emission appears in Figure 3d. This spectrum appears straight from 1.4 to 89 GHz with spectral index 1.34 ± 0.05. A comparison of Figure 1 with the 22.3 GHz map of Dreher (1981) shows that the spectrum of the diffuse emission in the Np and Sf lobes steepens rapidly away from their leading edges. This is to be expected, since the synchrotron lifetime of 89 GHz emitting electrons in the lobes is only about 8×10^4 yr, so that the electrons can only travel ∼10 arcsec before losing most of their energy.

By contrast, the spectrum of the central component is more complicated (Fig. 3c). Ignoring the single-dish flux densities, which lie well above the spectrum as measured by interferometers, it appears that the spectrum rises slowly from 1.6 to 6 GHz, then falls with spectral index 0.10 ± 0.03 to 89 GHz. The single-dish 21.7, 35, 99, and 150 GHz flux densities lie substantially above this spectrum, suggesting either that they contain some contribution from diffuse emission or that the central component is strongly variable at frequencies above 15 GHz. This latter possibility is unlikely, however, on the basis of two epochs of 23 GHz (Dreher 1979, 1981) and 89 GHz (this work; Birkinshaw and Wright 1982) observations, which yield substantially consistent flux densities.

The VLBI data (Kellermann *et al.* 1981; Linfield 1982) suggest that the central component of Cygnus A can be modeled as a ∼2 milli-arcsec core containing 0.6 Jy and a ∼2 × 5 milli-arcsec extension containing 0.4 Jy at 10.6 GHz. If we suppose that this structure can be regarded as a single component with angular size ∼3 milli-arcsec, we find that the spectrum of the central component of Cygnus A is well fitted with an homogeneous, isotropic, spherical model with an electron energy spectral slope, γ, of 1.25 and an electron gyrofrequency of about 5 GHz (a magnetic field of about 0.2 mT), so that the spectrum displays a synchrotron cutoff near 1.6 GHz. The magnetic field estimated from a minimum energy calculation is about 1.3 μT, considerably less than that estimated from the shape of the spectrum. This difference is probably due to the strong dependence of the magnetic field on the estimated, and very uncertain, angular size of the emitting region.

If we adopt a two-component model for the source, then a similar fit can be obtained for the magnetic fields in the core and the jet. Since the spectrum of the jet is not well constrained, we have assumed that it has spectral index 0.5, and that the core has spectral index 0.0. The spectrum can then be fitted with a synchrotron cutoff at ∼6 GHz in the core, and an optically thin spectrum at all observed frequencies for the jet. The corresponding magnetic field in the core is about 0.1 T; but if the angular size of the
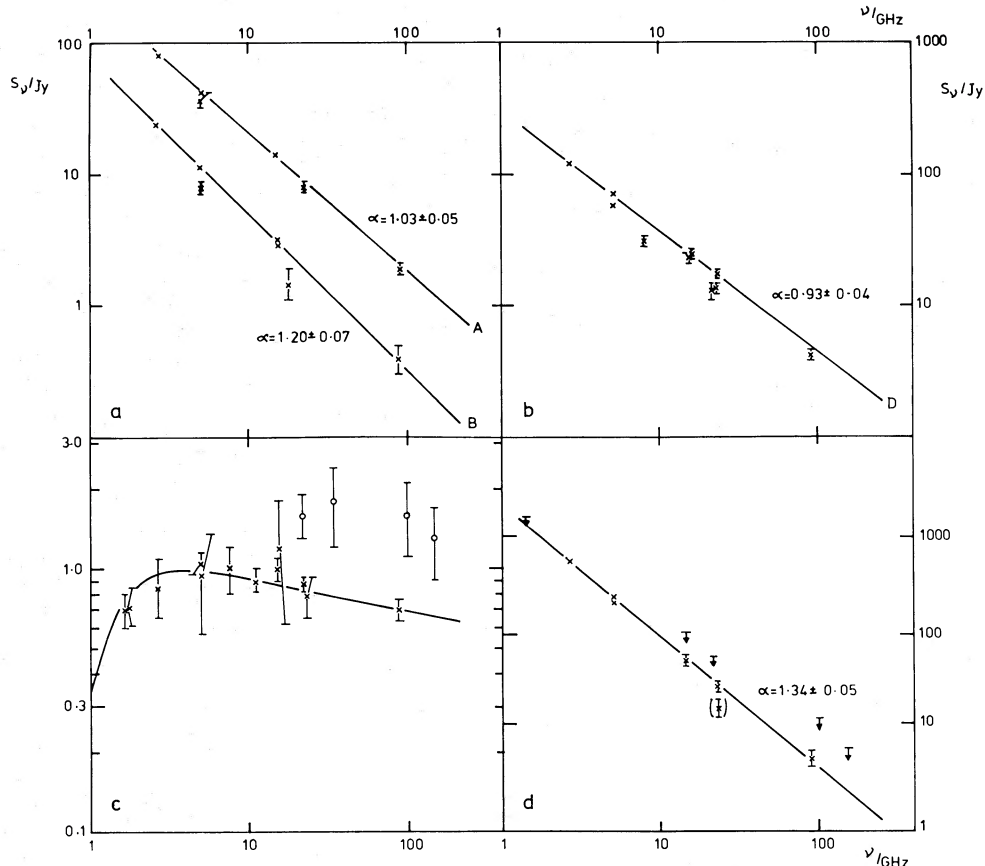
FIG. 3.—Spectra of the radio components at frequencies above 1.0 GHz. (a) A and B. (b) D. (c) Central. Single-dish flux density measurements are indicated by circles, and interferometric flux densities are indicated by crosses. A synchrotron spectrum with self-absorption cutoff near 1.6 GHz is shown for reference. (d) Sum of the diffuse emission of the Np and Sf lobes, with upper limits marked where the observations were of insufficient resolution to determine the contribution of the hot-spot components. The data are taken from Peckham (1973; 1.66 GHz), Bentley et al. (1975; 1.67 GHz), Alexander (1984; 2.7, 5.0, and 15.4 GHz), Hargrave and Ryle (1974, 1976; 5.0 and 15.4 GHz), Kellermann et al. (1975; 7.5 GHz), De Young, Hogg, and Wilkes 1979; 8.1 GHz), Linfield (1982; 10.6 GHz), Baker, Green, and Landecker (1975; 15.0 GHz), Berlin et al. (1980; 21.7 GHz), Dreher (1979, 1981; 23 and 22.3 GHz), Hachenberg et al. (1976; 35 GHz), this work (89 GHz), Hobbs et al. (1978; 99 GHz), and Kafatos et al. (1980; 150 GHz).

core is less than 0.5 milli-arcsec, the implied field drops below 1 mT.

These models for the central component may be checked by observations of its structure using VLBI at millimeter wavelengths and using VLBI at several centimetric wavelengths to examine the synchrotron cutoff expected to occur in the core at 6 GHz and in the jet at ~2 GHz.

V. CONCLUSIONS

From these observations we may conclude:

1. There is no evidence for 89 GHz variability of the central component over the 10-month interval of this synthesis. There is slight, but nonsignificant, evidence for such variability over the 3 yr interval between our 1980 and 1983 syntheses.

2. The hot spots show straight spectra with spectral indices 0.98 ± 0.02, significantly flatter than the lobe emission of 1.34 ± 0.05. No features corresponding to electron aging have been found.

3. The spectrum of the central component is well fitted by a simple model based on the VLBI structure, with core and jet magnetic fields less than about 1 mT.

REFERENCES

Alexander, P. 1984, in preparation.
Baars, J. W. M., Genzel, R., Pauliny-Toth, I. I. K., and Witzel, A. 1977, Astr. Ap., **61**, 99.
Baker, J. R., Green, A. J., and Landeker, T. L. 1975, Astr. Ap., **44**, 173.
Bentley, M., Haves, P., Spencer, R. E., and Stannard, D. 1975, M.N.R.A.S., **173**, 39P.
Berlin, A. B., Korenev, Yu. V., Lesovoj, V. Yu., Parijskij, Yu. N., Smirnov, V. I., and Soboleva, N. S. 1980, Soviet Astr. Letters, **6**, 260.
Birkinshaw, M., and Wright, M. C. H. 1982, in IAU Symposium 97, Extragalactic Radio Sources, ed. D. S. Heeschen and C. M. Wade (Dordrecht: Reidel), p. 27.

Blanford, R. D., and Rees, M. J. 1978, Phys. Scripta, **17**, 265.
De Young, D. S., Hogg, D. E., and Wilkes, C. T., 1979, Ap. J., **228**, 43.
Dreher, J. W. 1979, Ap. J., **230**, 687.
———. 1981, A.J., **86**, 833.
Fomalont, E. B., and Wright, M. C. H. 1974, in Galactic and Extragalactic Radio Astronomy, ed. G. L. Verschuur and K. I. Kellermann (Berlin: Springer), p. 256.
Gull, S. F., and Daniell, G. J. 1979, Nature, **272**, 686.
Hachenberg, O., Furst, E., Harth, W., Steffen, P., and Wilson, W. 1976, Ap. J. (Letters), **206**, L19.
Hargrave, P. J., and Ryle, M. 1974, M.N.R.A.S., **166**, 305.

Hargrave, P. J., and Ryle, M. 1976, *M.N.R.A.S.*, **175**, 481.
Hobbs, R. W., Maran, S. P., Kafatos, M., and Brown, L. W. 1978, *Ap. J. (Letters)*, **220**, L77.
Hogböm, J. A. 1974, *Astr. Ap. Suppl.*, **15**, 417.
Janssen, M. A., Golden, L. M., and Welch, W. J. 1974, *Astr. Ap.*, **33**, 373.
Kafatos, M. 1978, *Ap. J.*, **225**, 756.
Kafatos, M., Hobbs, R. W., Maran, S. P., and Brown, L. W. 1980, *Ap. J.*, **235**, 18.
Kellermann, K. I., Clark, B. G., Neill, A. S., and Shaffer, D. B. 1975, *Ap. J. (Letters)*, **197**, L113.
Kellermann, K. I., Downes, A. J. B., Pauliny-Toth, I. I. K., Preuss, E., Shaffer, D. B., and Witzel, A. 1981, *Astr. Ap.*, **97**, L1.

Linfield, R. 1982, *Ap. J.*, **254**, 465.
Peckham, R. J. 1973, *Nature Phys. Sci.*, **246**, 54.
Perley, R. A. 1983, in *IAU Symposium 110, VLBI and Compact Radio Sources*, in press.
Spinrad, H., and Stauffer, J. R. 1982, *M.N.R.A.S.*, **200**, 153.
Ulich, B. L. 1981, *A.J.*, **86**, 1619.
Welch, W. J., Forster, J. R., Dreher, J., Hoffman, W., Thornton, D. D., and Wright, M. C. H. 1977, *Astr. Ap.*, **59**, 379.
Winter, A. J. B., *et al.* 1980, *M.N.R.A.S.*, **192**, 931.

MARK BIRKINSHAW: Mullard Radio Astronomy Observatory, Cavendish Laboratory, Madingley Road, Cambridge CB3 0HE, England, UK

MELVYN C. H. WRIGHT: Radio Astronomy Laboratory, 601 Campbell Hall, University of California, Berkeley, CA 94720